Frequency Regulation using Data-Driven Controllers in Power Grids with Variable Inertia due to Renewable Energy

Patricia Hidalgo-Gonzalez^{†,‡,*}, Rodrigo Henriquez-Auba[†], Duncan S. Callaway^{†,‡} and Claire J. Tomlin[†]

Abstract—With the increasing penetration of non-synchronous variable renewable energy sources (RES) in power grids, the system's inertia decreases and varies over time, affecting the capability of current control schemes to handle frequency regulation. Providing virtual inertia to power systems has become an interesting topic of research, since it may provide a reasonable solution to address this new issue. However, power dynamics are usually modeled as time-invariant, without including the effect of varying inertia due to the presence of RES. This paper presents a framework to design a fixed learned controller based on datasets of optimal time-varying LQR controllers. In our scheme, we model power dynamics as a hybrid system with discrete modes representing different rotational inertia regimes of the grid. We test the performance of our controller in a twelvebus system using different fixed inertia modes. We also study our learned controller as the inertia changes over time. By adding virtual inertia we can guarantee stability of high-renewable (lowinertia) modes. The novelty of our work is to propose a design framework for a stable controller with fixed gains for timevarying power dynamics. This is relevant because it would be simpler to implement a proportional controller with fixed gains compared to a time-varying control.

Index Terms—Frequency Regulation, Renewable Energy, Data-Driven Controllers, Virtual Inertia Placement, Hybrid Systems.

I. INTRODUCTION

A mismatch between electricity generation and demand in a power system provokes a deviation in frequency from its nominal value. Different mechanisms exist in power systems to prevent or mitigate frequency excursions. The immediate response to frequency deviation comes from the inertial response of the grid. This inertial response originates from the kinetic energy supplied to the grid by the synchronous generators currently connected to it. This inertia (present in rotating masses of generators and turbines) determines the instantaneous change in frequency when imbalances of active power take place. More inertia in the system entails a slower rate of change of the frequency. Droop or governor response is the second mechanism that counteracts frequency deviations

P. Hidalgo-Gonzalez would like to thank the NSF Graduate Research Fellowships Program (GRFP). This work was also supported by NSF PIRE: Science of Design for Societal-Scale Cyber-Physical Systems (Award Number: UNIV59732), and by NSF awards 1539585 and 1646612.

[1]. Droop control is an automatic control proportional to the deviation in frequency. Slower mechanisms (e.g. spinning reserves) also participate to restore frequency to its nominal value [1].

Many countries have set ambitious goals to generate more electricity using renewable energy sources (RES) [2] and/or reduce their CO₂ emissions. This global trend will transform power systems from being fossil fuel dominated to being dominated by RES [3]. In this scenario, renewable sources, such as wind and solar, are usually connected to the grid through inverters, which decouple their rotational inertia (if existing) from the grid. Additionally, RES incorporate more uncertainty in electricity generation. This uncertainty can enhance the challenge of mitigating the mismatch between power generation and consumption, which increases the complexity of providing frequency regulation [4].

Generally, inverters do not provide inertial response to power systems. As the penetration of RES increases, the global inertia decreases and becomes strongly time-varying. This increases the variation of frequency under abrupt changes in generation and demand. This can lead to cases in which classical frequency control schemes are too slow to mitigate arising contingencies [5].

A possible solution for systems with low inertia is to use RES inverters or large scale storage to provide inertia. This can be done by operating the RES or storage's inverters as virtual inertia (control proportional to the derivative of the frequency), that could allow large penetration of RES without jeopardizing the system's stability [6]. Previous work studying virtual inertia can be found in the literature [7], [8], [9], [10], [11], and [12]. The literature around virtual inertia has focused on the effects on power systems with fixed low inertia over time and on the optimal allocation of virtual inertia controllers. Our earlier work [13], introduces a new modeling framework for power system dynamics to simulate a time-varying evolution of rotational inertia coefficients in the network. To do this, power dynamics are modeled as a hybrid system in which each mode corresponds to a rotational inertia regime. The novelty of this paper is the design of a fixed and stable frequency controller under a paradigm of time-varying inertia. We choose a fixed controller because it is simpler to implement (compared to a time dependent controller) given the existing droop control in the grid. In addition, the controller we propose does not require information about the current hybrid mode of the system or its uncertainty. Thus, our contributions

[†]P. Hidalgo-Gonzalez, R. Henriquez-Auba, D. S. Callaway and C. J. Tomlin are with the Department of Electrical Engineering and Computer Sciences, University of California, Berkeley, CA 94720, USA.

[‡]P. Hidalgo-Gonzalez and D. S. Callaway are also with the Energy and Resources Group, University of California, Berkeley, CA 94720, USA.

^{*}Corresponding author: patricia.hidalgo.g@berkeley.edu.

are the following:

- In the time-varying framework for power dynamics, we design a controller with fixed gains, proportional to the system's states (angles and frequencies). We design the controller by learning its parameters from the optimal control solution of a hybrid systems linear-quadratic regulator (LQR) formulation of power dynamics.
- For each mode of the hybrid system, we test the performance of the learned controller against the optimal time-varying controller from the LQR formulation.
- We add virtual inertia control (linear on the derivative of the frequency) to guarantee stability for all modes of the hybrid system when using the learned controller.

We conclude that for the hybrid power dynamics formulation it is possible to design, through learning, a static frequency controller proportional to the system's states that performs similarly to the optimal time-varying controller from LQR. It is possible to guarantee stability for the hybrid system when we add virtual inertia to the learned control.

The rest of the paper is organized as follows: Section II presents the problem formulation, Section III analyses stability of the hybrid system and shows the performance of the controller in different settings, and finally Section IV concludes with our main findings.

II. PROBLEM FORMULATION

A. Power grid dynamics as a hybrid system

We consider an electric power grid modeled as a graph with n nodes and n(n-1)/2 possible edges connecting them. The swing equation model, based on the direct current approximation [12], used for the network is given by

$$m_i \ddot{\theta}_i + d_i \dot{\theta} = p_{\text{in},i} - \sum_{j \in \mathcal{N}_i} b_{ij} (\theta_i - \theta_j), \quad i \in \{1, \dots, N\}$$
 (1)

where m_i corresponds to the equivalent rotational inertia in node i, d_i is the droop control, $p_{\text{in},i}$ represents power mismatch at node i, \mathcal{N}_i is set of nodes connected by an edge to node i, b_{ij} is the susceptance of the transmission line between nodes i and j, and θ_i is the voltage phase angle at node i. The state space representation of the model can be written as

$$\begin{bmatrix} \dot{\theta} \\ \dot{\omega} \end{bmatrix} = \begin{bmatrix} 0 & I \\ -M^{-1}L & -M^{-1}D \end{bmatrix} \begin{bmatrix} \theta \\ \omega \end{bmatrix} + \begin{bmatrix} 0 \\ M^{-1} \end{bmatrix} p_{\rm in} \quad (2)$$

where the states correspond to the stacked vector of angles and frequencies at each node $(\theta^\top, \omega^\top)^\top \in \mathbb{R}^{2n}$, $M = \operatorname{diag}(m_i)$ is a diagonal matrix with rotational inertia coefficients, $D = \operatorname{diag}(d_i)$ is a diagonal matrix with droop control coefficients, I is the $n \times n$ identity matrix, p_{in} corresponds to the power input, and $L \in \mathbb{R}^{n,n}$ is the Laplacian of the network. The network Laplacian is defined as $\ell_{ij} = -b_{ij}$ when $i \neq j$, and $\ell_{ii} = \sum_{j \in \mathcal{N}_i} b_{ij}$.

Thermal generators are predominant in the traditional paradigm of power systems. In this setting, the equivalent inertia can be considered as constant over time. However, due to the increasing penetration of RES, the equivalent rotational inertia has become lower and time-varying [5], [14]. This work

uses the modeling framework first introduced in [13] to represent the time dependence in inertia at each node. Frequency dynamics are modeled as a Switched-Affine hybrid system [15], where each mode has a predetermined set of values of equivalent inertia m_i at each node [13]. The evolution of the inertia on the system depends on the current online generators and the connected power electronics converter. In this paper, the inertia at each time step t evolves as an exogenous input over different modes. Thus, the power dynamics are given by

$$\begin{bmatrix} \dot{\theta} \\ \dot{\omega} \end{bmatrix} = \underbrace{\begin{bmatrix} 0 & I \\ -M_{q(t)}^{-1}L & -M_{q(t)}^{-1}D \end{bmatrix}}_{\hat{A}_{q(t)}} \begin{bmatrix} \theta \\ \omega \end{bmatrix} + \underbrace{\begin{bmatrix} 0 \\ M_{q(t)}^{-1} \end{bmatrix}}_{\hat{B}_{g(t)}} p_{\text{in}}$$
 (3)

where $M_{q(t)}$ represents the inertia matrix in the mode $q(t) \in \{1, \ldots, m\}$. Using a zero-order hold discretization with time step T_s , we obtain the discretized time-varying dynamics

$$x_{t+1} = A_{q(t)}x_t + B_{q(t)}u_t (4)$$

where x_t is the stacked vector of discretized angles and frequencies, $(\theta_t^\top, \omega_t^\top)^\top$, u_t is the control action by generators and converters, $A_{q(t)} = \exp(\hat{A}_{q(t)}T_s)$ and $B_{q(t)} = \int_0^{T_s} \exp(\hat{A}_{q(t)}\tau)\hat{B}_{q(t)}d\tau$.

In this paper, the switching between modes occurs between each time step, and it is given by a uniform distribution with the following possible outcomes: no change of inertia, increase of inertia, or decrease of inertia. For simplicity, for a given mode q we assume the same inertia coefficient for all nodes $M_q = m_q I_{n \times n}$. Using an LQR formulation we study the problem of returning to a steady-state configuration $x_{\rm ss}$, assuming a perturbed initial condition $x_0 \neq x_{\rm ss}$ due to a contingency.

B. Optimal frequency control for low and time-varying rotational inertia coefficients

To minimize an objective function where the states and controllers are decision variables we consider the LQR formulation

$$\min_{\boldsymbol{x}, \boldsymbol{u}} \sum_{t=0}^{T} x_{t}^{\top} Q x_{t} + u_{t}^{\top} R u_{t}$$
s.t. $x_{0} = x^{(0)}$

$$x_{t+1} = A_{q(t)} x_{t} + B_{q(t)} u_{t}, \ t \in \{0, T-1\}$$
(5)

where Q is a positive semidefinite matrix, R is a positive definite matrix, and $x^{(0)}$ is the initial state. Depending on the modeling goal, matrices Q and R can be modified to promote a specific behavior. The optimal solution of (5) for a fixed mode q in the entire time horizon (i.e. a linear time-invariant system) and with $T \to \infty$, can be found via the discrete time algebraic Ricatti equation [15]:

$$P_{q} = A_{q}^{\top} P_{q} A_{q} - A_{q}^{\top} P_{q} B_{q} (R + B_{q}^{\top} P_{q} B_{q})^{-1} B^{\top} P_{q} A_{q} + Q$$

$$K_{q} = (R + B_{q}^{\top} P_{q} B_{q})^{-1} B_{q}^{\top} P_{q} A_{q}$$

$$u_{t} = -K_{q} x_{t}$$
(6)

For a hybrid system with time-varying inertia, (5) is a Quadratic Programming problem that can be solved directly, using for example CVX [16]. We use the solution of (5) as a benchmark of an optimal controller for our problem.

C. Data-driven based controller

In the presented framework of variable inertia we are interested in learning a time-invariant controller of the form $u_t = -K_{\rm L} x_t$ where $K_{\rm L}$ is a constant matrix. The training dataset $(\boldsymbol{x}^{(k)}, \boldsymbol{u}^{(k)})$ we use comes from the optimal solution to (5) under different scenarios $k = \{1, \ldots, K\}$. The learning algorithm we use is least-squares:

$$\min_{K_{\rm L}} \sum_{k=1}^{K} \sum_{t=1}^{T} \left| \left| u_t^{(k)} - K_{\rm L} x_t^{(k)} \right| \right|_2^2 \tag{7}$$

It is interesting to notice that when we solve (5) for a single mode q (in the entire time horizon) and a sufficiently long time horizon T, least-squares returns the analytical solution K_q from the LQR problem (6). This is because the optimal controller from (5) is linear on the states, and with sufficient training data $(\boldsymbol{x}^{(k)}, \boldsymbol{u}^{(k)})$, (7) is a convex optimization program that achieves K_q , and hence the optimal value is equal to zero.

We assume a stressed case in which the equivalent inertia can change rapidly over time. Thus, inertia is allowed to change over time steps in each scenario. However, an equivalent training set can be generated by fixing the mode q at each scenario k, and only changing the mode between different scenarios. Each scenario in this training set would represent, for instance, a different hour of the year. During an hour, inertia could be considered fixed, and a different optimal controller would be obtained for each scenario.

D. Incorporating virtual inertia in the system

Depending on how we generate the training set $(\boldsymbol{x}^{(k)}, \boldsymbol{u}^{(k)})$, the controller we propose may not be stable in modes where the inertia is too low. The learned controller may not be fast enough to compensate the rate of change of the frequency. As an alternative, a controller that depends on the derivative of the frequency, $K_V\dot{\omega}$, can be used as a virtual inertia resource for the system. Indeed, consider the fixed inertia continuous time system and assume a controller of the form

$$u = -K_{\mathbf{L}}(\theta^{\top}, \omega^{\top})^{\top} - K_{\mathbf{V}}\dot{\omega} = -K_{\mathbf{L}}x - \tilde{K}_{\mathbf{V}}\dot{x}$$
(8)

where $\tilde{K}_{V} = [0 \ K_{V}]$, then:

$$\dot{x} = \begin{bmatrix} 0 & I \\ -M^{-1}L & -M^{-1}D \end{bmatrix} x - \begin{bmatrix} 0 \\ M^{-1} \end{bmatrix} (K_{L}x + \tilde{K}_{V}\dot{x})$$

Rearranging terms the system can be written

$$\dot{x} = (I + \hat{B}\tilde{K}_V)^{-1}(\hat{A} - \hat{B}K_L)x$$

$$= \begin{bmatrix} 0 & I \\ -\tilde{M}^{-1}(L + K_{L,\theta}) & -\tilde{M}^{-1}(D + K_{L,\omega}) \end{bmatrix} x$$

where $\tilde{M} = M(I + M^{-1}K_V) = M + K_V$ provides a new system wide equivalent inertia due to the virtual inertia

TABLE I PARAMETERS FOR THE TWELVE-BUS THREE-REGION CASE STUDY [11], [13] AND [17].

Parameter	Value
Transformer reactance	0.15 p.u.
Line impedance	(0.0001 + 0.001j) p.u./km
Base voltage	230 kV
Base power	100 MVA
Droop control	1.5 %/%

controller $K_{\rm V}$. To determine a proper $K_{\rm V}$ we develop a heuristic using a bisection method. We assume $K_{\rm V}$ of the form $K_{\rm V}=k_{\rm V}I_{n\times n}$. Iterating over $k_{\rm V}$, and assuming that $\dot x$ in the right hand side of the discretized system can be approximated by $[x_t-x_{t-1}]T_s^{-1}$, we modify $k_{\rm V}$ until the discretized closed loop system for the low inertia modes has all its eigenvalues inside the unit circle, making it stable.

III. SIMULATIONS AND RESULTS

A. Data description

Using MATLAB® we modeled a twelve-bus three-region network that has also been used in [11], [12], [13] and [17]. Each node has two states (angle and frequency). Table I shows the parameters of the network.

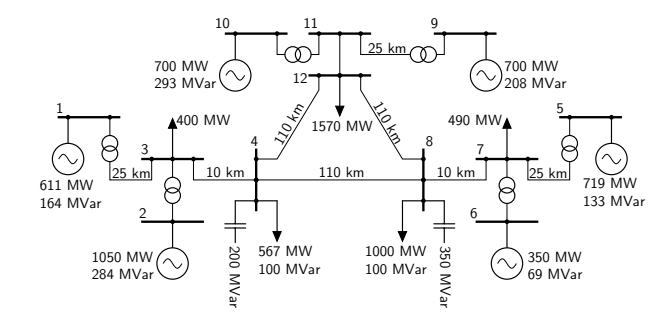


Fig. 1. Case study: Twelve-bus three-region network from [11], [12], [13] and [17].

We assume the same rotational inertia in all buses for a given time step t $(m_i(t) = m(t)$ for all i). This implies a similar fraction of renewable energy generation for all nodes, but this assumption can be easily extended. Each mode of the hybrid system is given by one value of inertia. For the study case we predefined possible inertia values for the system: $m_q \in \{0.2, 0.5, 1, 1.5, 2, 2.5, 3, 3.5, 5, 9\}$. The average of this set of possible inertia values is 2.8 seconds, which is equivalent to having 28 percent of thermal generation (10 s of inertia) and 72 percent of RES with zero inertia. Each simulation starts with 2 seconds of inertia (mode q_5), and from there– based on a uniform distribution draw- the inertia (hybrid mode) of the system at time t+1 will remain the same, increase, or decrease. In our simulations we only allow the possibility to change modes every 1, 4 or 10 time steps. For all the simulations we use a time step of $T_s = 0.01$ s. We generate K = 400scenarios of 7 seconds each (T = 700). The initial conditions we use in (5) are randomly drawn from a normal distribution

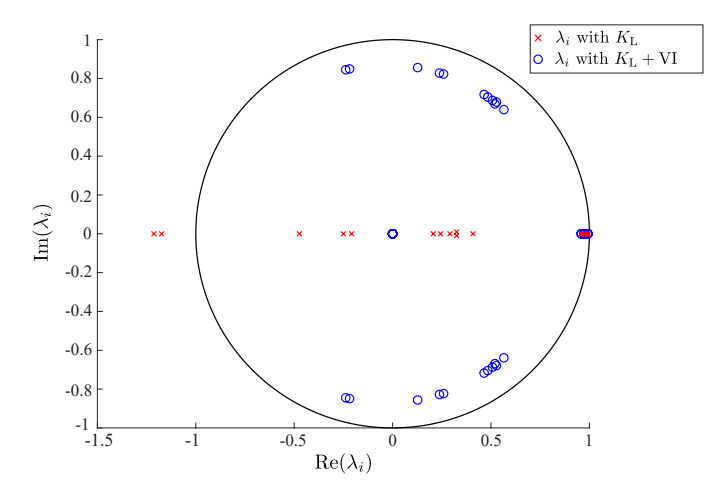


Fig. 2. Eigenvalue placement for the closed loop system in mode q_1 using the learned controller K_L (crosses) and adding virtual inertia control $K_L + VI$ (circles).

with zero mean and unitary variance. The training set we use to learn the controller K_L using (7) are the optimal solutions $(\boldsymbol{x}^{(k)}, \boldsymbol{u}^{(k)})$ from (5).

B. Stability analysis

The design of the controller $K_{\rm L}$ through learning provides a stable closed loop system $A_q-B_qK_{\rm L}$ for every mode except for q_1 . To correct this issue we use an approximated virtual inertia controller $\tilde{K}_{\rm V}(x_t-x_{t-1})T_s^{-1}$ with $\tilde{K}_{\rm V}=[0\ K_{\rm V}]$. The new dynamics can be written as:

$$\begin{aligned} x_{t+1} &= A_q x_t + B_q [-K_{\mathsf{L}} x + T_s^{-1} \tilde{K}_{\mathsf{V}} (x_t - x_{t-1})] \\ &= [A_q - B_q (K_{\mathsf{L}} - T_s^{-1} \tilde{K}_{\mathsf{V}})] x_t - T_s^{-1} B_q \tilde{K}_{\mathsf{V}} x_{t-1} \end{aligned}$$

Augmenting the states as $z_{t+1} = (x_t^\top, x_{t+1}^\top)^\top$, our new system can be written as:

$$z_{t+1} = \begin{bmatrix} 0_{2n \times 2n} & I_{2n \times 2n} \\ -T_s^{-1} B_q \tilde{K}_V & A_q - B_q (K_L - T_s^{-1} \tilde{K}_V) \end{bmatrix} z_t \quad (9)$$

For the learned controller, adding a virtual controller of the form $K_{\rm V}=0.15I_{n\times n}$ results in eigenvalues of the augmented system for mode q_1 inside the unitary circle. This is depicted in Figure 2, where it can be observed that there are two modes that are unstable for the closed loop system only using the learned controller (in red). When we incorporate the virtual inertia controller all modes are stable (in blue).

C. Controllers' comparison for fixed inertia

For each mode q, we compare the performance of the learned controller $K_{\rm L}$ and the learned controller with virtual inertia, $K_{\rm L}$ + VI, against the optimal controller from the LQR formulation. Table II shows peaks (ℓ_{∞} norm), ℓ_2 and ℓ_1 norms for frequency deviations f and control inputs u, and objective function values J for the different controllers under different inertia modes (columns). The values in table II represent increases in percentage with respect to the metrics for the LQR controller. The learned controller is unstable in the critical inertia regime (q_1 , lowest inertia). When adding virtual

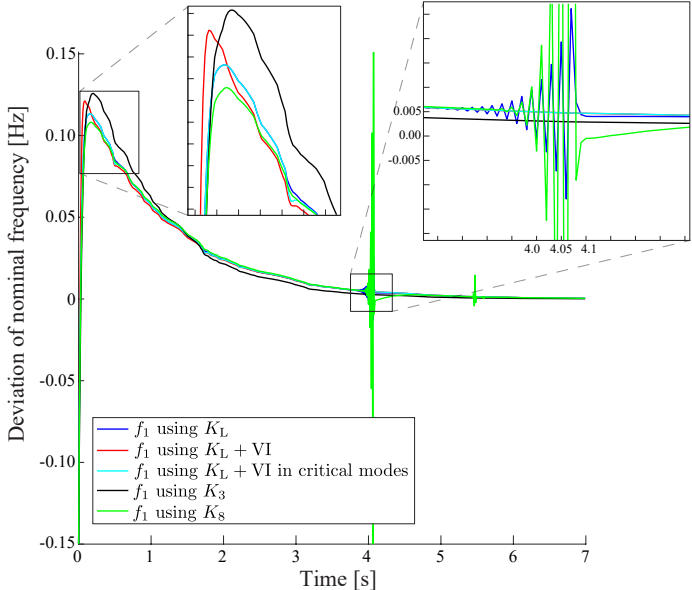


Fig. 3. Frequency deviations for node 1 for 5 different controllers from a hybrid system simulation.

inertia, the controller becomes stable. The objective values for the data-driven controllers are greater than for the LQR. This is intuitive because the learned controllers have fixed parameters over time while the LQR changes its parameters for each mode. The ℓ_2 norm for the frequency is in general smaller for the learned controllers than for the LQR controllers. On the other hand, the ℓ_2 norm of the control action is higher than in the LQR case.

D. Controllers' comparison for time-varying inertia

We evaluate the performance of different controllers in a simulation of the hybrid system switching among different inertia modes. We assume that the system starts in mode $q_2 = 0.5$ s, and possible transitions of inertia can occur every 4 time steps. Figure 3 depicts the evolution of frequency deviation in node 1, under 5 different controllers for an initial condition $f_0 = -0.15$ Hz at every node. The controllers we use are the following: In blue, the frequency is controlled using the learned controller K_L . In red, we show the learned and virtual inertia controller $K_L + VI$ (ensure stability). Similarly, cyan depicts a controller that uses $K_{\rm L}$ and virtual inertia only when the system is in the unstable mode q_1 . In black and green we use the optimal controllers K_q obtained from (6) for modes $q_3 = 1$ s and $q_8 = 5$ s, respectively. Around 4 seconds of the simulation, the system enters mode q_1 for around 0.4 seconds. This provokes an instability for controllers K_8 and K_L . After leaving the unstable mode the frequency is stabilized again. The other controllers are able to maintain stability in all the modes. In addition, key differences can be observed at the beginning of the simulation. Controller K_3 shows the highest overshoot of the simulation, while controller $K_L + VI$ (in red) is the fastest to peak due to the usage of the derivative of the frequency. Finally, the frequency for the first and third case (in

TABLE II COMPARISON OF LEARNED CONTROLLER (K_L) and learned controller with virtual inertia $(K_L + VI)$ against optimal control from LQR under different inertia modes

Metric	q_1	q_2	q_3	q_4	q_5	q_6	q_7	q_8	q_9	q_{10}
$ f_{K_{\mathrm{L}}} _{\infty}$	Unstable	-21.1%	-10.4%	-5.4%	-1.1%	2.6%	5.9%	8.8%	11.9%	14.4%
$ f_{K_{\rm L}+{\rm VI}} _{\infty}$	106.7%	-16.1%	-8.8%	-4.3%	-0.2%	3.5%	6.5%	9.5%	12.4%	14.4%
$ f_{K_{\rm L}} _2$	Unstable	-9.0%	-7.1%	-5.5%	-3.9%	-2.5%	-1.1%	0.2%	3.7%	11.2%
$ f_{K_{\mathrm{L}}+\mathrm{VI}} _2$	-7.2%	-8.9%	-7.4%	-5.8%	-4.3%	-2.9%	-1.5%	-0.3%	3.2%	10.9%
$ u_{K_{\rm L}} _{\infty}$	Unstable	3.2%	-2.7%	-5.9%	-8.2%	-10.2%	-11.9%	-13.3%	-17.1%	-15.2%
$ u_{K_{\rm L}+{ m VI}} _{\infty}$	87.9%	3.2%	-2.7%	-5.9%	-8.2%	-10.2%	-11.9%	-13.3%	-17.1%	-15.2%
$ u_{K_{\mathrm{L}}} _1$	Unstable	13.3%	6.2%	2.5%	-0.3%	-2.7%	-4.7%	-6.5%	-11.0%	-19.7%
$ u_{K_{\mathrm{L}}+\mathrm{VI}} _1$	78.1%	19.0%	8.6%	4.2%	1.1%	-1.4%	-3.6%	-5.5%	-10.2%	-19.1%
$ u_{K_{\mathrm{L}}} _2$	Unstable	12.2%	6.0%	4.6%	4.4%	4.6%	4.9%	5.3%	6.5%	9.2%
$ u_{K_{\mathrm{L}}+\mathrm{VI}} _2$	45.2%	16.4%	8.7%	6.6%	5.9%	5.8%	5.9%	6.1%	7.1%	9.4%
$J_{K_{ m L}}$	Unstable	29.8%	39.9%	49.2%	57.8%	65.7%	73.2%	80.2%	98.9%	138.1%
$J_{K_{\rm L}+{ m VI}}$	39.1%	31.6%	40.2%	49.0%	57.4%	65.3%	72.6%	79.5%	98.1%	137.3%

blue and cyan) are almost identical except when the system is in the mode q_1 . This shows that if we can detect when the system is in critical modes, we can apply virtual inertia control only when it is necessary to obtain a better performance.

IV. CONCLUSIONS

In this paper we propose a new framework for obtaining a constant data-driven controller for uncertain and time-varying power system dynamics. This is relevant because it can be intractable to solve frequency dynamics in real time (time-varying LQR) in large power networks. In addition, time-varying controllers, as the one from LQR, rely in the ability to predict or identify the current mode of the hybrid system. Finally, given the existing infrastructure and droop control, it would be simpler to implement a proportional controller with fixed gains compared to a time-varying control.

We use a switched affine hybrid system, where its modes change based on the changes of inertia in the system [13], we find optimal controllers using an LQR formulation. We use the solution (x, u) from the LQR as a dataset to train a fixed controller. We test our learned controller in different modes against optimal controllers. Results show that our learned controller can be used to obtain a similar performance as the optimal LQR controllers in the different modes. Finally, we show that adding a virtual inertia controller can stabilize the system for low inertia modes. This highlights the importance of using more flexible controllers when considering temporal variability in the system dynamics. For future work we plan to explore the performance of our controller with AC power flow, voltage dynamics, machine dynamics and power electronics (inverters) approximate dynamics. We will also compare our proposed controller with a robust controller. We also plan to study different learning algorithms with new features to test the efficiency of the learned controller, in particular promoting sparsity and information requirements using LASSO or Block Sparse Regression.

REFERENCES

[1] E. Ela, M. Milligan, and B. Kirby, "Operating reserves and variable generation," *Nat. Renew. Energy Lab., Golden, CO, USA*, Aug 2011.

- [2] J. Notenboom, P. Boot, R. Koelemeijer, and J. Ros, "Climate and Energy Roadmaps towards 2050 in north-western Europe: A concise overview of long-term climate and energy policies in Belgium, Denmark, France, Germany, the Netherlands and the United Kingdom," PBL Netherlands Environmental Assessment Agency, Netherlands, Tech. Rep., 2012.
- [3] M. Wei, J. Nelson, M. Ting, C. Yang, D. Kammen, C. Jones, A. Mileva, J. Johnston, and R. Bharvirkar, "California's carbon challenge: Scenarios for achieving 80% emissions reductions in 2050," *Lawrence Berkeley National Laboratory, UC Berkeley, UC Davis, and Itron to the California Energy Commission*, 2012.
- [4] U.S. Department of Energy (DOE), "Maintaining Reliability in the Modern Power System." 2016.
- [5] A. Ulbig, T. S. Borsche, and G. Andersson, "Impact of low rotational inertia on power system stability and operation," *IFAC Proceedings Volumes*, vol. 47, no. 3, pp. 7290–7297, 2014.
- [6] H. Bevrani, T. Ise, and Y. Miura, "Virtual synchronous generators: A survey and new perspectives," *International Journal of Electrical Power* & Energy Systems, vol. 54, pp. 244–254, 2014.
- [7] U. Tamrakar, D. Shrestha, M. Maharjan, B. P. Bhattarai, T. M. Hansen, and R. Tonkoski, "Virtual inertia: Current trends and future directions," *Applied Sciences*, vol. 7, no. 7, p. 654, 2017.
- [8] Q.-C. Zhong and G. Weiss, "Synchronverters: Inverters that mimic synchronous generators," *IEEE Transactions on Industrial Electronics*, vol. 58, no. 4, pp. 1259–1267, 2011.
- [9] E. Mallada, "idroop: A dynamic droop controller to decouple power grid's steady-state and dynamic performance," in 2016 IEEE 55th Conference on Decision and Control (CDC), Dec 2016, pp. 4957–4964.
- [10] A. Ulbig, T. Rinke, S. Chatzivasileiadis, and G. Andersson, "Predictive control for real-time frequency regulation and rotational inertia provision in power systems," in *Decision and Control (CDC)*, 2013 IEEE 52nd Annual Conference on. IEEE, 2013, pp. 2946–2953.
- [11] T. S. Borsche, T. Liu, and D. J. Hill, "Effects of rotational inertia on power system damping and frequency transients," in *Decision and Control (CDC)*, 2015 54th IEEE Conference on. IEEE, Dec 2015, pp. 5940–5946.
- [12] B. K. Poolla, S. Bolognani, and F. Dörfler, "Optimal placement of virtual inertia in power grids," *IEEE Transactions on Automatic Control*, vol. 62, no. 12, pp. 6209–6220, 2017.
- [13] P. Hidalgo-Gonzalez, D. S. Callaway, R. Dobbe, R. Henriquez-Auba, and C. J. Tomlin, "Frequency regulation in hybrid power dynamics with variable and low inertia due to renewable energy," in 2018 IEEE Conference on Decision and Control (CDC), Dec 2018, pp. 1592–1597.
- [14] Electricity Reliability Council of Texas (ERCOT), "Future ancillary services in ERCOT," ERCOT: Taylor, TX, USA, 2013.
- [15] F. Borrelli, A. Bemporad, and M. Morari, "Predictive control for linear and hybrid systems," *Cambridge University Press*, 2017.
- [16] M. Grant and S. Boyd, "CVX: Matlab software for disciplined convex programming, version 2.1," http://cvxr.com/cvx, Mar. 2014.
- [17] P. Kundur, "Power system stability and control," McGraw-Hill, 1994.
- [18] MATLAB, version 9.4 (R2018a). Natick, Massachusetts: The Mathworks, Inc., 2018.